Summer student report 2023

on the topic

ISOLDE summer student report Commissioning of the MULTIPAC detectors

by

Björn Dörschel[2]

Supervisor:	Juliana Schell[1,2]
Co- supervisor:	Ian Chang Jie Yap[1]
Date:	26.06.2023

[1]Institute for Material Science and Center for Nanointegration Duisburg-Essen (CENIDE), University of Duisburg-Essen, Essen, Germany
[2]European Organization for Nuclear Research (CERN), Geneva, Switzerland

Contents

Abstract

The MULTIPAC project, located at the ISOLDE experimental hall at CERN, aims to revolutionize the measurement of magnetic properties in materials. Most of today's technology relies on magnetic components. To create more efficient components, better magnetic materials must be discovered and studied. To achieve this, the MULTIPAC project has developed a unique construction capable of performing vibrating sample magnetometry (VSM) and perturbed angular correlation spectroscopy (PAC). The combination of these two methods will allow the investigation of local and macroscopic magnetic properties in materials. The VSM aspect of the MULTIPAC project is already operational, while the PAC spectroscopy is currently in the construction phase. For this purpose, the detectors have been built and tested.

Ackowledgement

The CERN summer student program offers an incredible and valuable opportunity that every scientist should aspire to experience. In general, there's a lot to learn about physics, even without actively working on your project. However, the most captivating aspect of the summer student program is, of course, the opportunity to participate in a project based at CERN. I was fortunate to work on the ISOLDE experiment within the MULTIPAC project.

Throughout my physics studies at my home university, I gained a substantial amount of knowledge. Still, it's an entirely different experience to work on such a significant project that is at the forefront of current research. Thanks to my supervisor, Juliana, and my teammates, Ian and Magnus, I had the chance to learn extensively, gain valuable experience, and contribute to the project's success. Working in a radioactive environment and with multimillion-dollar equipment is an experience I will never forget. I am profoundly grateful for the opportunity that Juliana provided me to be a part of her project.

My heartfelt appreciation goes to my teammates, Ian and Magnus. We encountered numerous setbacks during our project, and there were truly challenging days when nothing seemed to work. Therefore, seeing the detectors operational was an even more significant achievement.

We thank the the support received from the Federal Ministry of Education and Research (BMBF) under grants 05K16PGA, 05K22PGA and 05K22PGB. We also thank the European Union's Horizon Europe Framework research and innovation programme under grant agreement no. 101057511 (EURO-LABS).

Chapter 1

Introduction

The MULTIPAC [1][2] project is extremely unique worldwide. It is the first project capable of performing vibrating sample magnetometry (VSM) and perturbed angular correlation (PAC) spectroscopy without moving the sample. Moreover, it can be conducted at temperatures ranging from 3 K to 375 K and under an external magnetic field of up to 8.5 Tesla. Both VSM and PAC techniques are used to quantify the magnetic properties of samples. VSM is employed to determine magnetic susceptibility, magnetic moment, coercivity, and remanence. By varying the temperature, the sample undergoes phase transitions, allowing the characterization of its properties in different phases such as ferromagnetic or paramagnetic. These properties are derived by measuring the hysteresis curve via VSM [3].

PAC can derive the local properties of a material by measuring the hyperfine interactions, which results from the coupling of nuclear moments and their interaction with the first neighbours of the nuclear probe. The hyperfine structure depends on atomic environmental factors such as local structure, defects, impurities, crystal symmetry, and electronic properties [4][5][6]. Similarly, as in VSM, all of these properties can be determined under different phases.

The primary objective of the MULTIPAC project is to study samples using radioactive isotopes produced by the ISOLDE-CERN facility [7][8]. This will be done to chatacterize new materials, as nanoscale magnetic materials have a wide range of applications.

To conduct all these measurements, the main task is to ensure the detectors work properly and to calibrate them accurately. To achieve this, the detectors for PAC spectroscopy had to be constructed and tested before being integrated into the MULTIPAC setup.

Chapter 2

Measurements Techniques

This chapter will introduce two measurement techniques: the Vibrating-Sample Magnetometer (VSM) and Perturbed Angular Correlation (PAC). VSM will be briefly discussed, as its functionality has already been extensively tested, so the focus will be on providing a detailed explanation of PAC.

2.1 Vibrating-Sample Magnetometer

The VSM operates on the principles of Faraday's Law of Induction. Figure 2.1 illustrates the schematic of a VSM measurement.

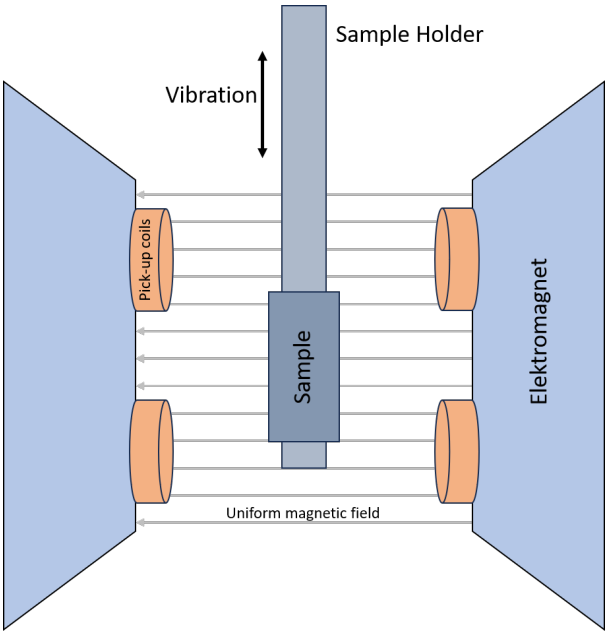

Figure 2.1: Schematic of the VSM measurement

Two external magnets generate a uniform magnetic field. When a magnetic sample is introduced into this field, its magnetization aligns parallel to the uniform magnetic field. The sample is connected to a piezoelectric material, allowing it to vibrate vertically. This vertical movement induces a time-dependent magnetic field within the sample due to the magnetic dipole moments. The final component of VSM measurements involves pickup coils. According to Faraday's Law of Induction, the time-dependent magnetic field induces an electric field in these pickup coils. The measured current in the coil is proportional to the magnetization of the sample. By varying the strength of the uniform magnetic field, we can record a hysteresis curve, which can then be analyzed to determine the magnetic properties of the sample [3].

2.2 Perturbed Angular Correlation

To perform a PAC measurement, the radioactive isotope called as "PAC probe" must be incorporated inside a crystal lattice. The isotope must decay via a cascade of two gammas and the intermediate state between the two gammas is the time window of the PAC measurement. Typically, the gammas are emitted in different directions, necessitating the use of multiple detectors, such as six detectors arranged in an octahedral configuration [9]. When PAC detects a start-stop spectrum pair, it is referred to a coincidence and is associated with a specific spectra representing the angle between the detecting detectors. The number of spectra Z can be calculated using the permutation formula [10]:

$$P(n,k) = \frac{n!}{(n-k)!} \tag{2.1}$$

Here, n is representing the number of total detectors and k represents the number of detectors involved in a detection. Since we are trying to figure out the number of possible start-stop spectrum pairs, k is equal to 2. In our case, with six detectors, this leads to 30 spectra. Due to the law of radioactive decay, the signal follows an exponential curve. The nucleus exhibits non-spherically symmetric radiation, resulting in interaction with the surrounding electrical and magnetic fields. This interaction introduces periodic disorder known as the hyperfine interaction.

Such a process is shown in fig. 2.2. There is a PAC setup shown with two detectors. These two detectors do a coincidence measurement.

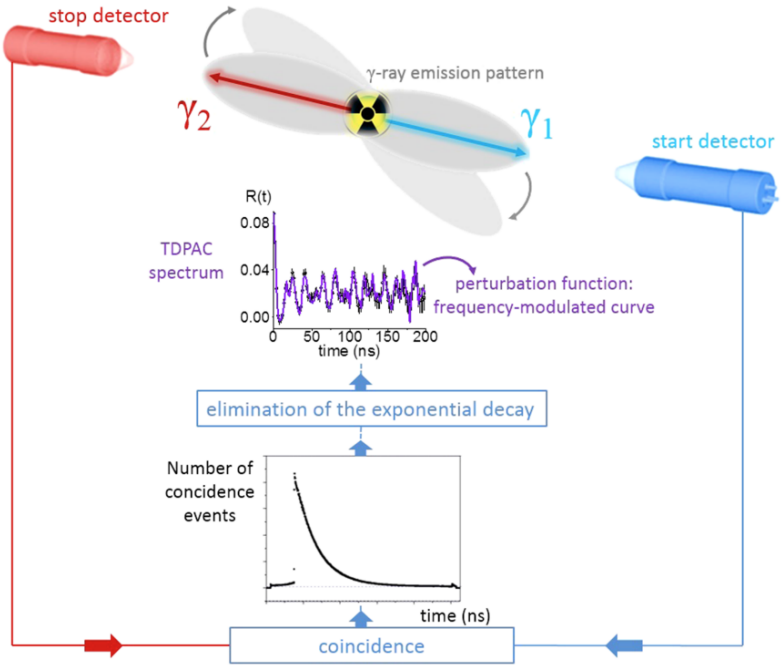

Figure 2.2: Measurement process of a PAC spectroscopy. (Reproduced from [11] under the Creative Commons Attribution 4.0 (CC BY) licenses. Copyright 2017 under Schell, J. et al.

To obtain the PAC spectra, the coincidence spectra for an angle between the detectors of 90° and 180° are interpolated. When interpolating the spectra, the exponential functions and detector properties cancel out, leaving only the PAC spectra (as seen in fig.2.2), denoted as $R(t)$, as follows [12]:

$$R(t) = 2\frac{W(180°, t) - W(90°, t)}{W(180°, t) + 2W(90°, t)} \tag{2.2}$$

$R(t)$ contains all information about the hyperfine interaction such as: electric quadrupol frequency, hyperfine magnetic frequency, asymmetry parameter, electric field gradients, damping factor from local environments and many more. From that, the local structure, the phase transitions and other properties of the material can be characterized.

Chapter 3

Detector

This is the main part of the present study—a detector setup for PAC spectroscopy for MULTIPAC was designed, constructed, and tested. First of all, the detector parts will be explained, then the construction process, and finally, the in-depth testing of the detectors to ensure their proper functionality. For the PAC spectroscopy in MULTIPAC, a total of four or six detectors are needed [13]. However, these should keep their functionality upon the application of a magnetic field.

3.1 Detector Parts

The detector consists mainly of four parts: the $LaBr_3$ (Ce) [14] scintillator crystal, the MPPC/SiPM [15][16], the MPPC circuit board, and the U5310A digitizer [17]. In the following, the function of all parts will be explained along with their exact specifications, leading to the answer of why these parts were chosen for MULTIPAC. The construction of the detectors from the individual parts can be seen in Appendix A.

3.1.1 $LaBr_3$ (Ce) Scintillator

A scintillator absorbs radiation (in our case, gamma radiation). The absorbed radiation will excite multiple electrons in the scintillator. When the electrons return to their ground state, they emit photons in a cascade. This means the scintillator transforms the high-energy gammas into multiple low-energy photons.
The $LaBr_3$ (Ce) scintillator is an inorganic crystal lattice structure that consists of Lanthanum (La) and Bromide (Br) [14]. Cerium atoms are implanted as a dopant impurity in this crystal.

In this scintillator, the electrons in the Cerium atoms are responsible for scintillation, meaning they get excited by the gamma's energy. Lanthanum Bromide acts like a matrix for Cerium atoms, efficiently transferring the absorbed gammas energy to the Cerium atoms. After the Cerium electrons get excited, they return to their ground state and emit the same energy as needed for excitation (scintillation). The energy needed for excitation is lower than the energy of the gammas, leading to multiple excited Cerium atoms and the transformation of one high-energy gamma into multiple low-energy photons. This is called the Light yield and is given in [photons/gamma energy keV]. The Light yield for $LaBr_3$ (Ce) is very high with 63, that means for 1keV of gamma energy there will be produced on average 63 photons [14].

The crystal structure of Lanthanum Bromide has an excellent radiation hardness. Furthermore, the arrangement of the atoms in the structure is clear and precisely defined. This enables very efficient energy transport throughout the crystal, resulting in excellent energy and time resolution. Cerium is a stable chemical element and when implanted in Lanthanum Bromide, it also exhibits high stability, which can be seen in the high density of 5.2 g/cm^3 and a high melting point of 1116 C°. Additionally, Cerium has high energy transport capabilities, meaning it can easily absorb energy and is capable of absorbing gammas. The reflection loss is only 6.8% [14].

In combination, these elements add up to a scintillator with really suitable specifications for PAC spectroscopy. It has a high light output of 63,000 photons per MeV, a good energy resolution of 2.6% at 662 keV, and a fast decay time of 25 ns on average. The high photon output leads to a more sensitive scintillator, improving the signal-to-noise ratio. This results in high accuracy even with low-energy gammas. The good energy resolution gives us the possibility to distinguish precisely between different energy levels. The fast decay time means that after a gamma hits the scintillator crystal, it needs 25 ns until the energy gets emitted. That means two gammas that reach the scintillator crystal in a time interval of more than 25 ns can be distinguished. In total, we get a very sensitive scintillator with high accuracy and very good time and energy resolution [14].

3.1.2 Silicon Photomultiplier

After gammas produce photons in the $LaBr_3$ (Ce) scintillator, the next step involves detecting these photons. However, a challenge arises as the photons likely have low energy. To address this, a photomultiplier (PM) becomes valuable in detecting low-energy photons. Nevertheless, the use of a conventional PM is unsuitable for MULTIPAC. MULTIPAC aims to operate and yield results under magnetic fields, but regular PMs are not immune to

magnetic fields, leading to inaccurate results. To overcome this limitation, Silicon photomultipliers (SiPMs) are employed. The primary material in SiPMs is silicon, which is immune to magnetic fields. Another important information, is that a SiPM produces a positive signal, whereas a regular PM produces a negative signal [18].

When a low-energy photon strikes the silicon material of the SiPM, it generates electron-hole pairs within the silicon through the photoelectric effect. The energy of these photons remains unchanged; it is simply converted into an electronic signal. The SiPM comprises a matrix of tiny avalanche photodiodes (APDs), each consisting of a PN junction, connected in parallel. Each APD operates in avalanche mode, wherein the detection of a single photon triggers a cascade of electron-hole pairs through an avalanche process (see fig. 3.1) [19].

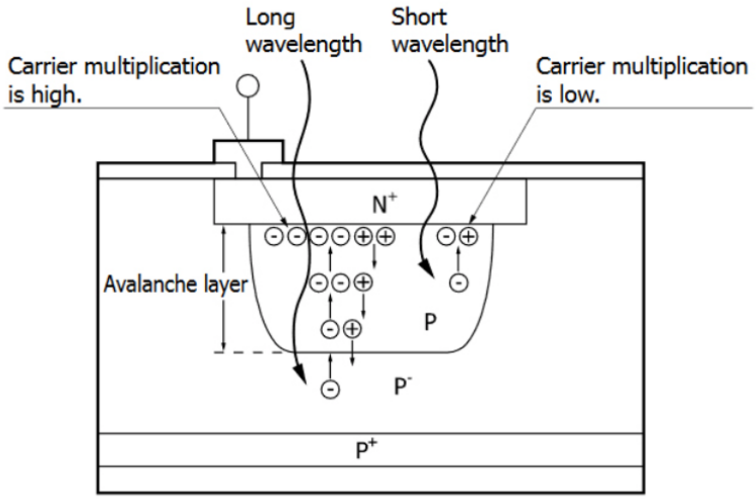

Figure 3.1: Avalanche mode of an avalanche photodiode. For long and short wavelengths. [19]

The avalanche process amplifies the initial signal produced by the photon. This multiplication of charge results in a measurable electrical pulse. The electrical pulses generated by each APD in response to the photons are then summed up. The collective signal is proportional to the number of detected photons, enabling the measurement of low-intensity light [18].

The specific SiPM used is Hamamatsu S13361-6050 [20] SiPM. This SiPM consists of 16 photosensitive areas, each with 16 individual channels. Each channel comprises 14336 pixels, all capable of separately detecting a

single photon. The advantages of this SiPM include a high gain of $1.7 \cdot 10^6$, signifying that a single photon initiates an avalanche, creating $1.7 \cdot 10^6$ photons. Additionally, the photo detection efficiency (PDE), indicating the probability of detecting a photon, is 40%, which is very high. The dark count, representing how many signals the SiPM produces in the absence of photons, is $2 \cdot 10^6$ per second. In comparison to the gain, and when divided by the total pixel value, the dark count is minimal. This results in a very good signal-to-noise ratio. The last important value is the breakdown voltage, at which voltage the SiPM should be operated, which is 53 ± 5 volts [20].

3.1.3 SiPM Circuit Board

The SiPM circuit board is custom-designed to meet the specific specifications of the SiPM. It consists of 16 signal readers, each dedicated to capturing signals from the 16 photosensitive areas on the SiPM. Each signal reader is equipped with four capacitors, enhancing the recovery time. This feature facilitates the rapid capture of signals within a shorter time period, resulting in improved time resolution.

Due to the sensitivity of the SiPM avalanche to temperature variations, the circuit board includes a built-in temperature sensor. The current temperature can be transmitted to the voltage supply, which should feature a built-in temperature compensation. Maintaining a consistent output for the same energy level of gammas is crucial for result comparison and ensuring constant energy levels throughout the measurement duration. However, the temperature changes in the $LaBr_3$ (Ce) scintillator, caused by heating of technical components, can impact the avalanche output. By adjusting the voltage in response to temperature fluctuations, a stable avalanche can be maintained even under changing temperatures for the SiPM.

3.1.4 U5310A Digitizer

A digitizer converts an analog signal into a digital signal. An analog signal is continuous, meaning it has a specific value at every point in time. However, for a computer, dealing with an infinite amount of data is impractical. Therefore, to bring the signal into a computer, it needs to be discretized, a process, which is done by a digitizer. Achieving more detailed information from the analog signal requires a fine level of discretization.

The U5310A digitizer [17] has a sample rate of 10 GS/s, indicating that 10 billion samples are taken every second. This leads to a time discretization of 100 ps. This high sample rate results in an exceptionally detailed digital signal. Furthermore, the digitizer can be set to operate simultaneously, transforming

two signals at the same time, each with a sample rate of 5 GS/s. While time is discretized, the amplitude values must also undergo discretization. The U5310A digitizer offers a 10-bit resolution, meaning the analog amplitude values are divided into 2^{10} digital values [17].

Given that the U5310A digitizer has a range of 1 volt, more than sufficient for PAC spectroscopy, the discretization for the amplitude values (denoted as N) is calculated as follows:

$$N = \frac{1\,\text{Volt}}{2^{10}} = 0.0001\,\text{Volt} \tag{3.1}$$

This level of discretization is highly favorable. In summary, the U5310A digitizer's discretization is very small, resulting in an exceptionally detailed digital signal. This level of detail is crucial in PAC spectroscopy to observe every aspect of the hyperfine interaction structure[17].

3.2 Detector Testing

The exact setup for the detector testing can be seen in Appendix B. To test the detectors, we decided to use Cobalt 60 as a calibration source [21]. The Cobalt 60 source is sealed, so that no alpha and beta particles could be spilled. The probability that it decays into two times excited Nickel is very high at 99.88% (see Fig. 3.2). Since we need two gammas, which indicate the start and stop signals for PAC, it is a suitable source to test our PAC spectroscopy detectors.

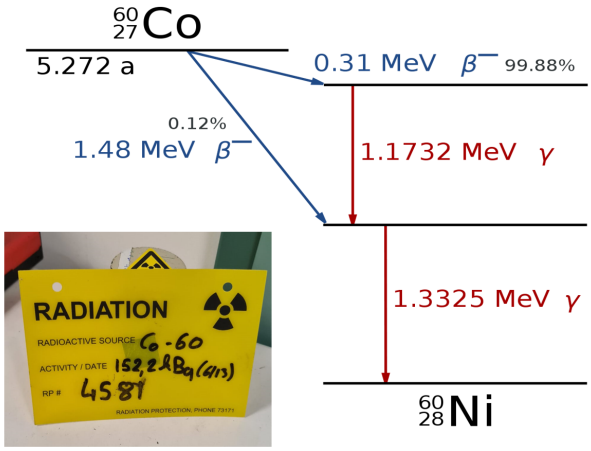

Figure 3.2: The decay scheme of Cobalt 60, and in the bottom left, how the probe was sealed with the exact specifications [22].

To test the detectors properly, we had to ensure that no background lights at all reached the detectors; otherwise, it could lead to an overcurrent. For that, we created a black box to put the detector inside. To be absolutely sure that no light would reach the detector, we covered the black box with a big black blanket. The Cobalt 60 and the detector were placed inside the black box and covered with the black blanket. First, a measurement with an oscilloscope was carried out. This was done to ensure that all parts in the detector and cables were functioning correctly. After some technical issues, a signal with the oscilloscope could be detected. In Fig. 3.3, the oscilloscope signal can be seen. The first signal is the signal from the γ-ray. As expected, the signal goes really high up and then decreases exponentially. The second signal is not created by a γ-ray, it is created due to aftertalk, which is an undesired effect.

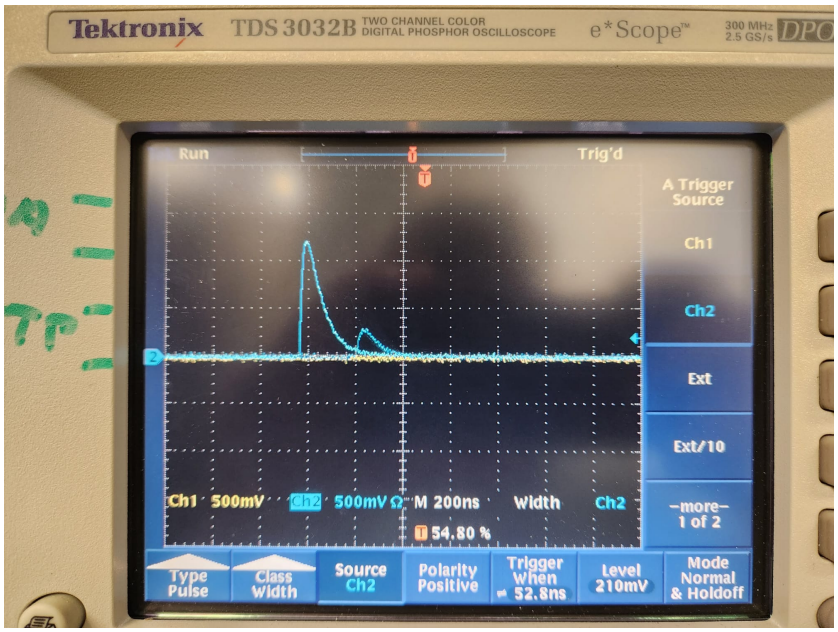

Figure 3.3: Detected signal from the Cobalt 60 with the detector shown on an oscilloscope.

After we were sure that all pieces worked properly, it was time to connect the detector to the digitizer and measure multiple signals over a certain time period (seen in Fig. 3.4). The digitizer signals look the same as in the oscilloscope. It has the same characteristic exponential decrease. On the y-axis is the voltage in millivolts, and on the x-axis is the time in nanoseconds. The height of the different curves represents that multiple gammas or other particles that can excite electrons in the scintillator hit our detector at the

same time.

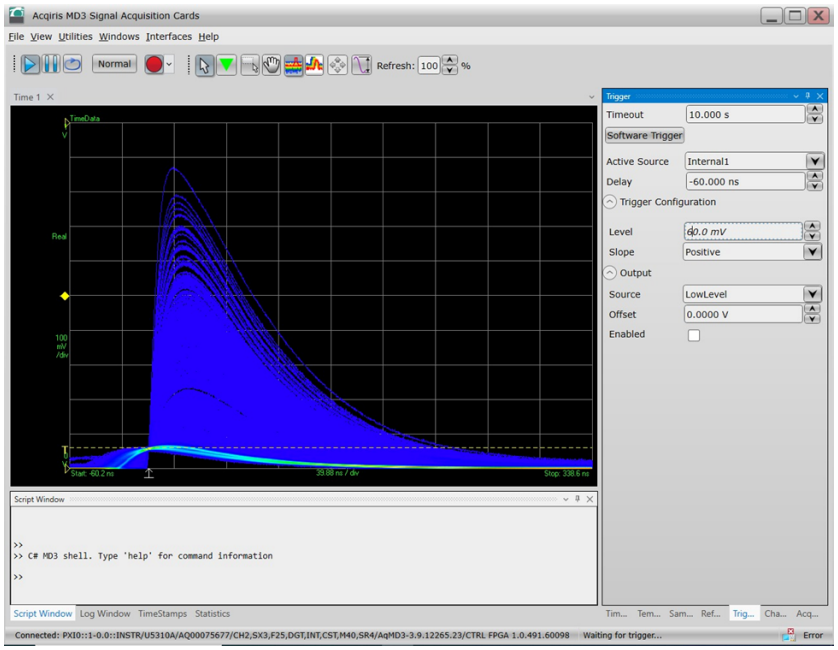

Figure 3.4: Detection of multiple signals from the detector and plotted by the digitizer software Acqiris. Every curve gives out a txt file.

Since the curve is time against voltage, it means that the integration over the curve gives the charge. From the produced txt files, the charge for every curve was calculated. This charged gets normalized with the intrinsic resistance value from the SiPM. It was not possible to get or determine this value from the SiPM. The only thing that is known, is that this value is constant. But that is not a problem for the experiment, since we just want to distinguish the energy peaks. The distribution of the normalized charged then can be plotted (see Fig. 3.5), since the true value of R_q is not available, the plot does not represent the true charge.

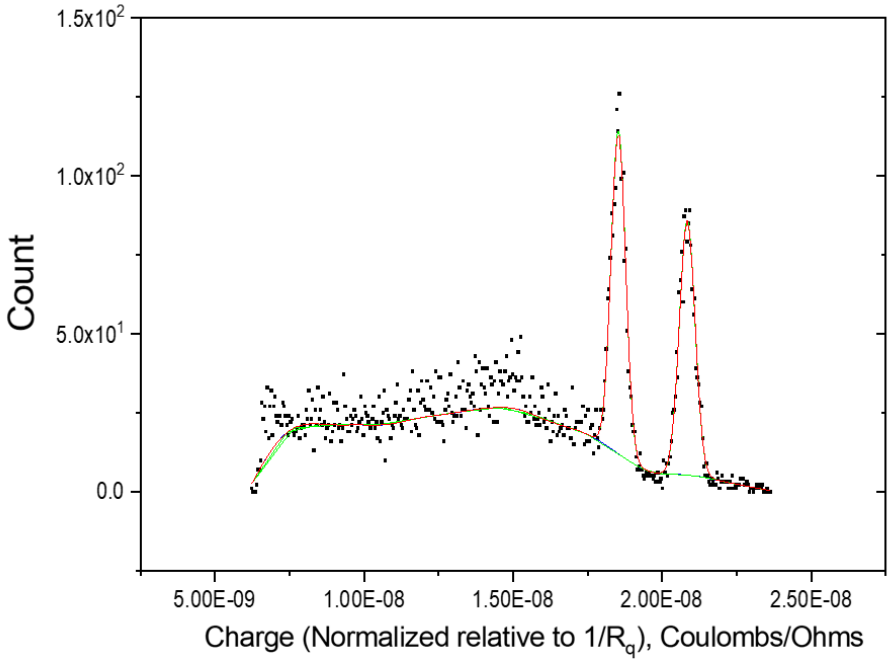

Figure 3.5: Plot of the not true normalized charge distribution. The two peaks were fitted with a Gaussian and a smoothed background in OriginPro [23]. The FWHM is red-marked, since it is the most important value.

Peak	Peak Type	FWHM	Max Height	Center Gravity
Left	Gaussian	5.72×10^{-10}	101.97664	1.85×10^{-09}
Right	Gaussian	6.18×10^{-10}	80.53881	2.08×10^{-08}

Table 3.1: Fitting Parameters

In the plot, two main peaks can be identified. These two peaks represent the two gammas with different energy emitted by the Cobalt 60 source. By fitting the fits and calculating the full-width-half-maximum (FWHM) [21][13], the energy resolution of the detector can be identified. The two peaks were fitted with a Gaussian, and the FWHM was calculated (red marked in fig. 3.5). The next step would be to obtain the time resolution. The plan for this is to conduct additional measurements with a time stamp, and by filtering out gamma rays with incorrect energies, a coincidence search is done. This is followed by plotting a histogram of the time difference between the timestamps of the two detectors.Sadly, my time at CERN ended before we could achieve this. But I am happy that I can still be involved in the project,

and I am looking forward to see where the project goes and to read the next MULTIPAC report from Magnus.

Several technical challenges were encountered during the testing phase, necessitating the use of special cables, and some cables proved to be ineffective. This led to an intensive error search, requiring the replacement of each part to ensure proper functionality. Additionally, multiple overcurrents were observed, resulting from excessive ambient light exposure to the detector. Furthermore, issues arose with the MPPC circuit board, which posed a challenge as the board was customized, and initial access to the schematics was limited. However, with time and the acquisition of the correct schematics, all problems were resolved, confirming the proper operation of the detector.

Chapter 4

Conclusion and Outlook

The detector was successfully assembled from individual components, and its functionality was verified. Subsequently, the detector effectively transmitted signals to a digitizer, and the resulting signals were successfully plotted. This marked a crucial initial step toward calculating the energy resolution of the entire detector. Unfortunately, due to various technical issues encountered during detector testing, there was insufficient time to gather the necessary data for an exact energy resolution calculation.

The next steps involve gathering more data to evaluate the energy resolution of the detectors. Following this, the determination of time resolution becomes another crucial task. Once these two quantities are calculated, measurements involving multiple detectors can be conducted. After confirming the functionality of several detectors, such as four or six, a correlation measurement can be pursued—a significant step toward conducting actual PAC spectroscopy.

However, before engaging in PAC spectroscopy, adjustments to the software are necessary. The current software for PAC spectroscopy is designed for photomultiplier tubes (PMT), which operates with a negative bias. In contrast, SiPMs operate with a positive bias, introducing a discrepancy in the software that needs to be addressed and corrected.

Bibliography

[1] Doru Lupascu et al. *MULTIPAC-Setup for gamma-gamma Perturbed Angular Correlation Experiments in Multiferroic (and Magnetic) Materials*. Tech. rep. Geneva: CERN, 2020. URL: https://cds.cern.ch/record/2706092.

[2] Juliana Schell et al. *MULTIPAC-Setup for Perturbed Angular Correlation Experiments in Multiferroic (and Magnetic) Materials: proof-of-concept*. Tech. rep. Geneva: CERN, 2023. URL: https://cds.cern.ch/record/2845935.

[3] Simon Foner. "Versatile and Sensitive Vibrating-Sample Magnetometer". In: *Review of Scientific Instruments* 30.7 (Dec. 2004), pp. 548–557. ISSN: 0034-6748. DOI: 10.1063/1.1716679. eprint: https://pubs.aip.org/aip/rsi/article-pdf/30/7/548/8344446/548_1_online.pdf. URL: https://doi.org/10.1063/1.1716679.

[4] Günter Schatz and Alois Weidinger. "Nuclear Condensed Matter Physics: Nuclear Methods and Applications". In: 1995, pp. 997–1044. URL: https://api.semanticscholar.org/CorpusID:117339032.

[5] K. Siegbahn. *Alpha-, Beta- and Gamma-ray Spectroscopy*. Bd. 2. NHPC, 1968. URL: https://books.google.be/books?id=pB5XxwEACAAJ.

[6] A. Abragam and R. V. Pound. "Influence of Electric and Magnetic Fields on Angular Correlations". In: *Phys. Rev.* 92 (4 Nov. 1953), pp. 943–962. DOI: 10.1103/PhysRev.92.943. URL: https://link.aps.org/doi/10.1103/PhysRev.92.943.

[7] R Catherall et al. "The ISOLDE facility". In: *Journal of Physics G: Nuclear and Particle Physics* 44.9 (Aug. 2017), p. 094002. DOI: 10.1088/1361-6471/aa7eba. URL: https://dx.doi.org/10.1088/1361-6471/aa7eba.

[8] Karl Johnston et al. "The solid state physics programme at ISOLDE: recent developments and perspectives". In: *Journal of Physics G: Nuclear and Particle Physics* 44.10 (Aug. 2017), p. 104001. DOI: 10.1088/1361-6471/aa81ac. URL: https://dx.doi.org/10.1088/1361-6471/aa81ac.

[9] Ulrich Gonser. *Microscopic Methods in Metals*. Springer Berlin, Heidelberg, 2012, p. 317. URL: https://doi.org/10.1007/978-3-642-46571-0.

[10] Eric Weisstein. *Permutation – from Wolfram MathWorld*. https://mathworld.wolfram.com/Permutation.html. Jan. 2024.

[11] Juliana Schell, Peter Schaaf, and Doru C. Lupascu. "Perturbed angular correlations at ISOLDE: A 40 years young technique". In: *AIP Advances* 7.10 (Oct. 2017), p. 105017. ISSN: 2158-3226. DOI: 10.1063/1.4994249. eprint: https://pubs.aip.org/aip/adv/article-pdf/doi/10.1063/1.4994249/12898449/105017_1_online.pdf. URL: https://doi.org/10.1063/1.4994249.

[12] Matthew Zacate and Herbert Jaeger. "Perturbed Angular Correlation Spectroscopy – A Tool for the Study of Defects and Diffusion at the Atomic Scale". In: *Defect and Diffusion Forum* 311 (Mar. 2011), pp. 3–38. DOI: 10.4028/www.scientific.net/DDF.311.3.

[13] Matthias Nagl et al. "A new all-digital time differential y-y angular correlation spectrometer". In: *Review of Scientific Instruments* 81.7 (July 2010), p. 073501. ISSN: 0034-6748. DOI: 10.1063/1.3455186. eprint: https://pubs.aip.org/aip/rsi/article-pdf/doi/10.1063/1.3455186/15691369/073501_1_online.pdf. URL: https://doi.org/10.1063/1.3455186.

[14] Advatech. *LaBr3(Ce) - Lanthanum Bromide (Ce) Scinillator Crystal*. URL: https://www.advatech-uk.co.uk/labr3_ce.html.

[15] HAMAMATSU - PHOTON IS OUR BUSINESS. URL: https://www.hamamatsu.com/eu/en/product/optical-sensors/mppc.html.

[16] Nagl & Vetter GmbH. *Die Nagl & Vetter GmbH – mehr als ein Entwicklungsdienstleister*. URL: https://nagl-vetter.de/de/.

[17] Acqiris. *U5310A 10-bit ADC Card - from 5 GS/s to 10 GS/s, with real-time processing*. URL: https://acqiris.com/hardware/10-bit/.

[18] HAMAMATSU - PHOTON IS OUR BUSINESS. URL: https://hub.hamamatsu.com/us/en/technical-notes/mppc-sipms/what-is-an-SiPM-and-how-does-it-work.html#:~:text=A%20SiPM%20is%20a%20pixelated,an%20anode%20and%20a%20cathode.

[19] HAMAMATSU - PHOTON IS OUR BUSINESS. Also sections 1-4 are used. URL: https://hub.hamamatsu.com/us/en/technical-notes/mppc-sipms/a-technical-guide-to-silicon-photomutlipliers-MPPC-Section-1.html.

[20] HAMAMATSU - PHOTON IS OUR BUSINESS. URL: https://hep.hamamatsu.com/content/dam/hamamatsu-photonics/sites/documents/99_SALES_LIBRARY/ssd/s13361-6050_series_kapd1056e.pdf.

[21] M. A. M. Nagl. "Next-Generation Perturbed Angular Correlation Spectroscopy". PhD thesis. University Göttingen, 2014.

[22] Wikipedia. *Zerfallsschema — Wikipedia, die freie Enzyklopädie*. [Online; Stand 19. November 2023]. 2023. URL: https://de.wikipedia.org/w/index.php?title=Zerfallsschema&oldid=232473849.

[23] *Origin(Pro)*. Version 2022. Northampton, MA, USA: OriginLab Corporation.

Appendix A

Step 1: The SiMP is glued to the $LaBr_3$ (Ce) scintillator with optical grease. It is glued in the middle of the side where the crystal is visible through the glass. It is better with less optical grease. Wait for some minutes for the optical grease to dry.

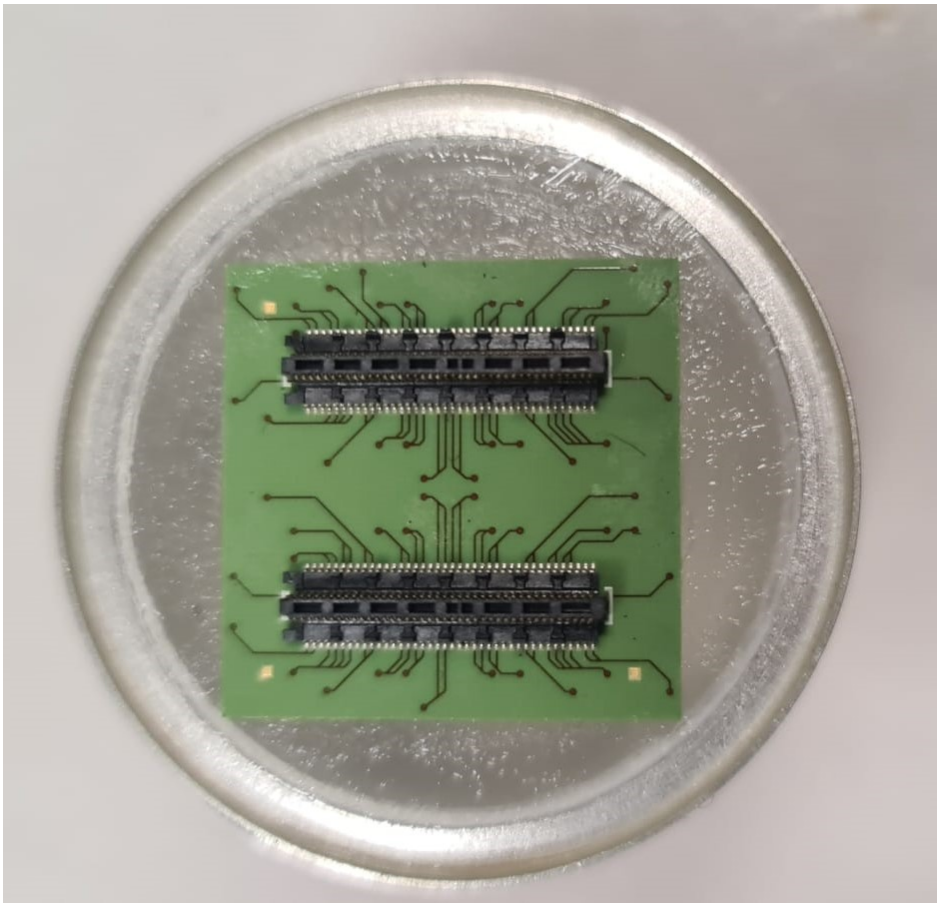

Figure A.1: MPPC glued on the $LaBr_3$ (Ce)) scintillator crystal on the glass side

Step 2: The surrounding of the SiPM, so the rest of the glass, gets covered by a red piece of plastic to minimize the light that hits the $LaBr_3$ (Ce) scintillator.

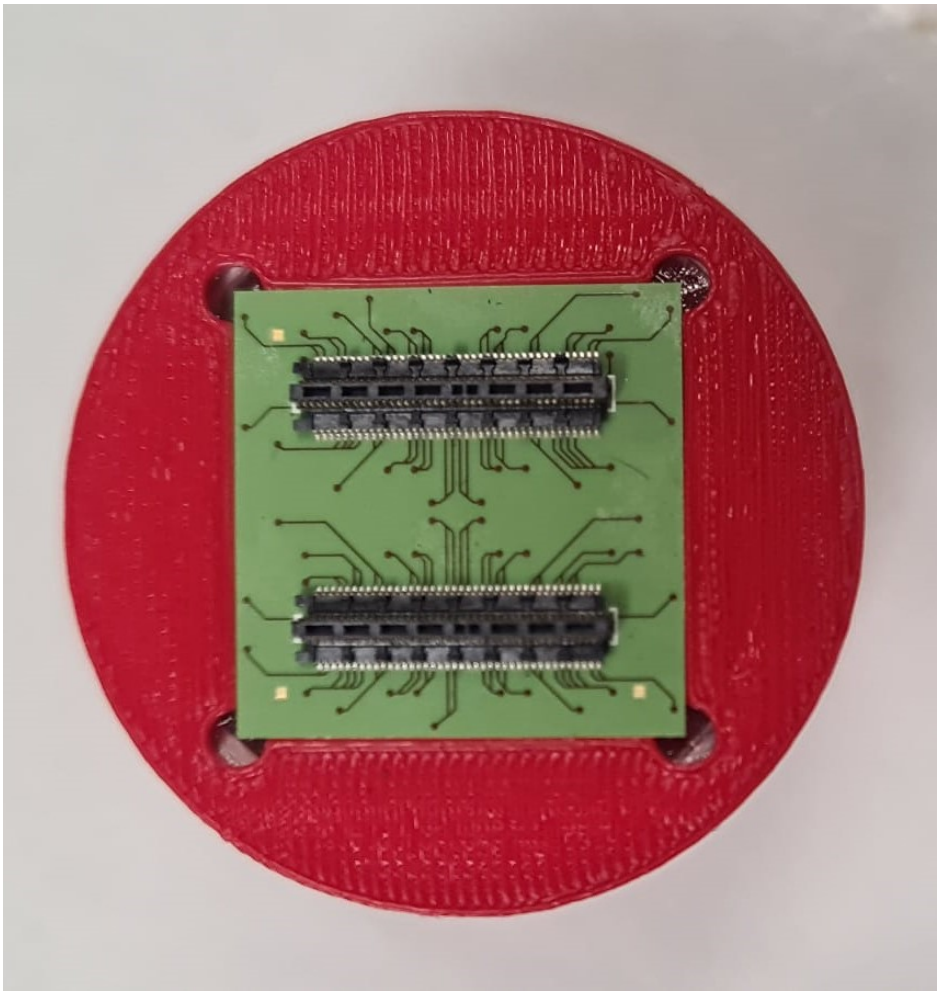

Figure A.2: Red plastic piece placed around MPPC on $LaBr_3$ (Ce) scintillator crystal on the glass side.

Step 3: To both of the flat sides of the $LaBr_3$ (Ce) scintillator, a red plastic object is attached. This is used to secure the SiPM, and it is used to mount the detector later. On the opposite side of the SiPM, the gamma photons will penetrate through the metallic-colored material, which surrounds the $LaBr_3$ (Ce) scintillator crystal.

Figure A.3: Two red plastic objects got stuck on the $LaBr_3$ (Ce) scintillator crystal. Also, the side for the gamma photon penetration is visible.

Step 4: The MPPC circuit board gets placed carefully on the SiPM.

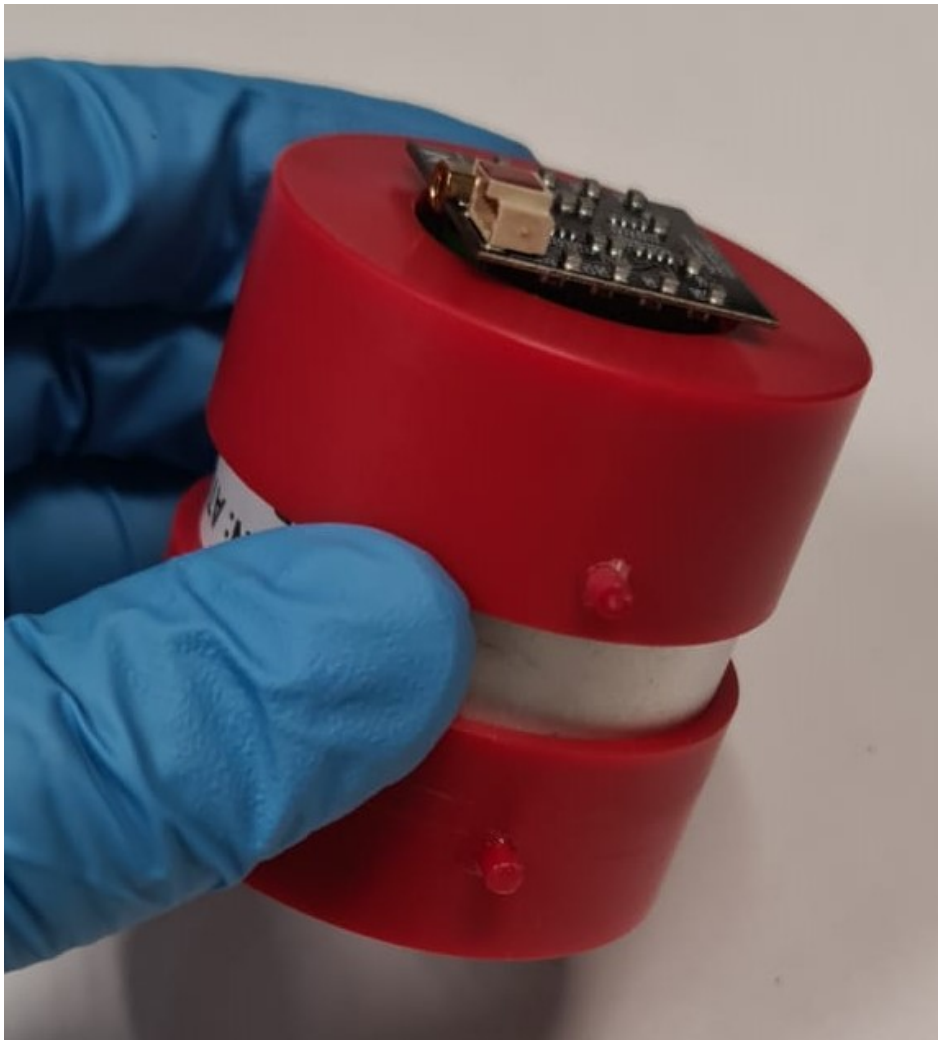

Figure A.4: The MPPC circuit board got placed on the MPPC.

Step 5: The MPPC gets connected to the U5310A digitizer and to a voltage supply.

Figure A.5: Fully constructed detector connected to the U5310A digitizer and to a voltage supply.

Appendix B

Step 1: A black box was designed to protect the LaBr3 (Ce) scintillator from light. It is filled with black-colored foam to protect the detector from vibration and motion.

Figure B.1: Opened black box, filled with black foam, and ceiling laying next to it.

Step 2: The detector and the cobalt 60 source are placed in the black box. The detector is placed in the direction so that the opposite side of the SiPM shows to the cobalt 60 source.

Figure B.2: Opened black box with detector and cobalt 60 source inside.

Step 3: The black box is closed, be careful not to squeeze the cables.

Figure B.3: Closed black box with detector and cobalt 60 source inside; the cables are going out.

Step 4: The black box is covered by a black blanket to ensure that absolutely no light hits the detector.

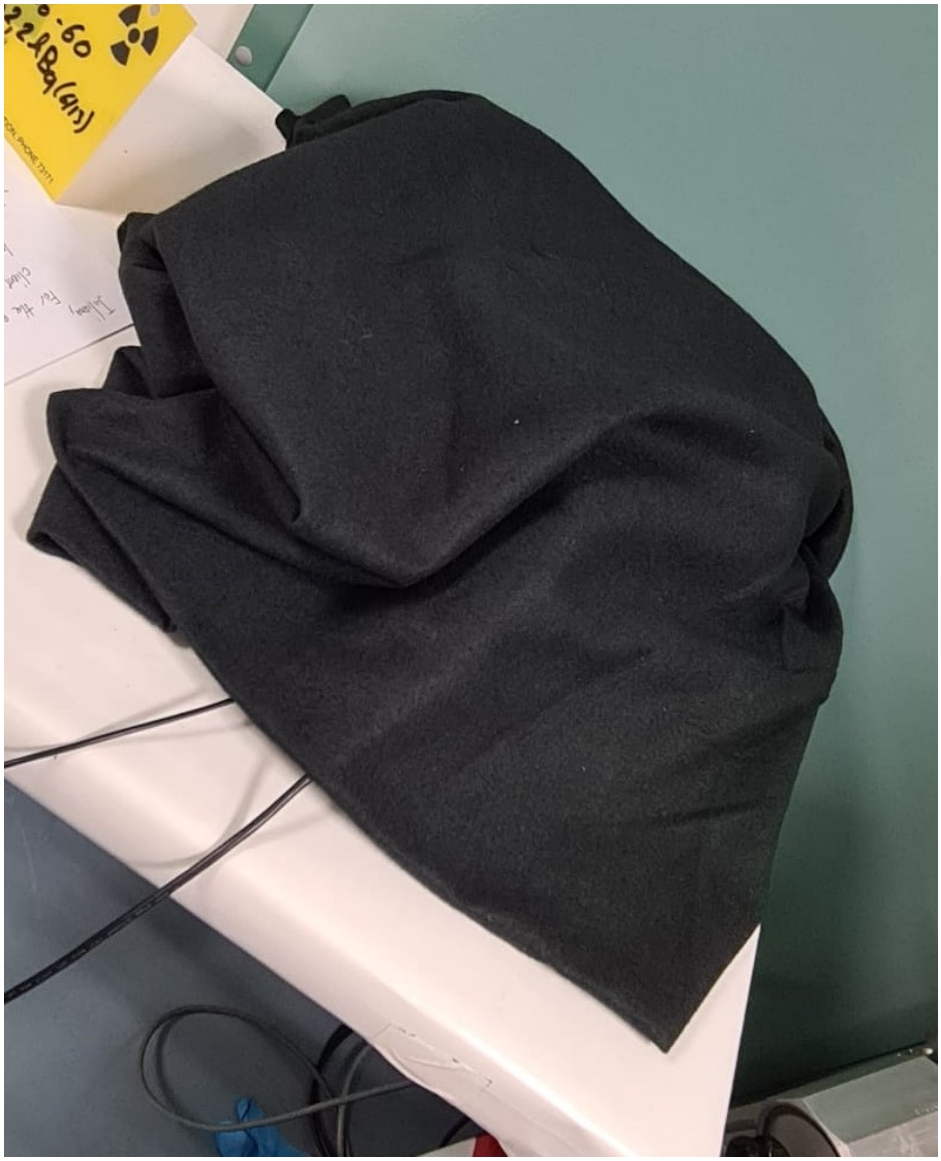

Figure B.4: Black box covered with a black blanket; the cables from the detector are still visible.

Step 5: The voltage supply is turned on at around 54 Volts [20] since the SiPM is most efficient at that voltage. Moreover, temperature compensation should be turned on too, as the avalanche of the SiPM is highly sensitive to temperature changes. So the voltage automatically changes regarding temperature changes to ensure the same avalanche output for the same gamma photon energy but under different temperatures.

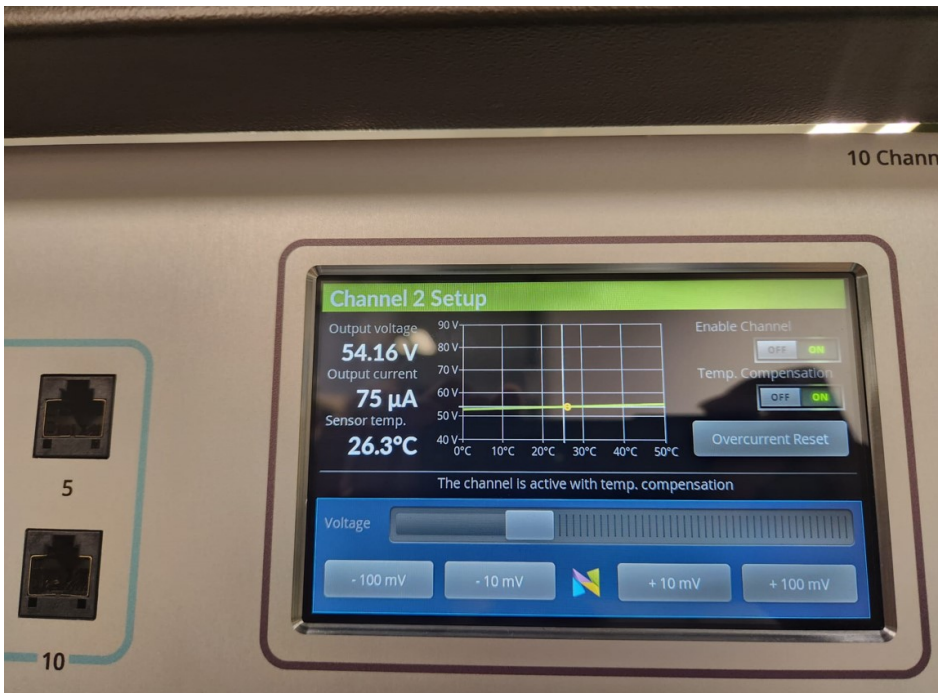

Figure B.5: Voltage supply for the detector with temperature compensation.

Step 6: Multiple signals can be measured and plotted in a voltage (millivolt) against time (nanosecond) curve by the digitizer.

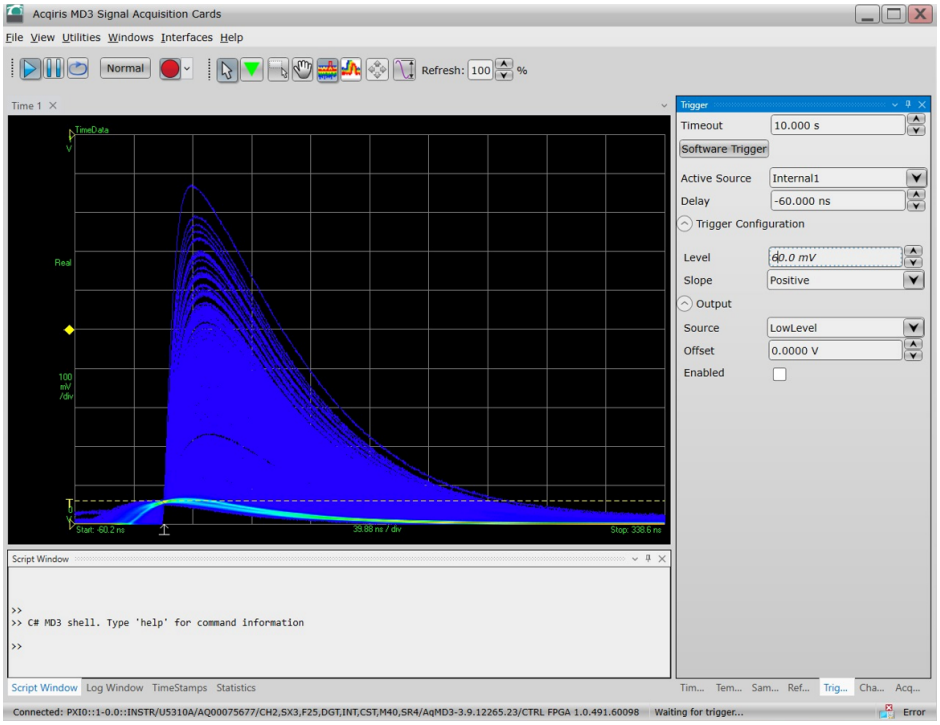

Figure B.6: Software Acqiris to plot data from the digitizer in a voltage (millivolt) against time (nanosecond) curve.